Alleviating avalanche effects in low-voltage grids: an analysis of novel grid charge options for residential customers

Oliver Resch *, Bianca Illing *, Leo Semmelmann *, Christof Weinhardt*
*Karlsruhe Institute of Technology, Institute of Information Systems, Karlsruhe, Germany
{oliver.resch, bianca.illing, leo.semmelmann, weinhardt}@kit.edu

***Abstract*—The increasing electrification of residential energy consumption, combined with dynamic electricity tariffs, raises concerns about potential overloads in low-voltage distribution grids. Through a simulation study combining empirical household data and thermal building models, we analyze how different grid charge structures affect grid stability under varying dynamic tariff adoption rates. We find that while traditional volumetric charges lead to significant overloads at high adoption rates, both peak-level and three-tier segmented charges effectively maintain grid stability, suggesting their potential as policy instruments for grid management.**

***Index Terms*—demand response, grid charges, energy policy, thermal model**

I. Introduction

European lawmakers have mandated large electricity suppliers to offer dynamic electricity pricing alongside existing fixed-rate options, aiming to align household consumption with power system scarcity signals [1]. While this policy supports Europe's renewable energy transition, simultaneous consumer responses to these uniform price signals could overwhelm electrical distribution grids [2], [3]. This risk is particularly relevant as households increasingly adopt flexible loads like electric vehicles and heat pumps, highlighting the importance of developing specialized models to evaluate how various grid charge policies could help maintain grid stability.

A. Motivation

Europe's energy transition is a cornerstone of its climate change mitigation strategy, with renewables playing a pivotal role [4] and expected to grow significantly [5]. To manage the intermittent nature of these renewables, demand response—the adjustment of electricity consumption to match supply—is enabled through EU-proposed [1] dynamic electricity tariffs. These provide incentives for implicit demand response in the form of price signals to consumers [6].

The electrification of transport and residential heating is driving increased adoption of large, flexible devices like electric vehicles (EVs) and heat pumps in households [7]. Home energy management systems (HEMS) automate the coordination of these devices, optimizing electricity consumption for cost-efficiency [8]. By leveraging dynamic tariffs, HEMS can align significant portions of residential electricity demand with power system scarcity signals.

979-8-3315-1278-1/25/$31.00 © 2025 IEEE European Union

This growing flexibility, however, introduces new challenges: synchronized responses from multiple flexible devices to a common price signal can cause significant fluctuations in aggregated load, potentially exceeding local grid capacity and increasing the risk of overloads—referred to as the avalanche effect [9]. Even without demand response, similar risks arise from simultaneous EV charging during peak evening hours, further stressing distribution networks [10], [11].

B. Related work

The impact of tariff structures on grid stability has been widely studied, particularly in the context of electric vehicle charging and decentralized flexibility options. A recurring finding is that volumetric electricity tariffs and standard grid charges can lead to significant reinforcement costs due to load synchronization effects, especially when EV charging follows uniform price signals, causing peak load congestion [10].

Dynamic tariff schemes have been analyzed for their influence on consumption patterns, as they introduce price signals that can incentivize load shifting. However, research indicates that while these tariffs provide marginal economic benefits to consumers, they may also contribute to herding behavior, where users respond similarly to price fluctuations, exacerbating grid congestion [12]. To mitigate these effects, distribution system operators (DSOs) may need to implement additional intervention strategies.

Beyond EV charging, decentralized flexibility options such as thermal energy storage and battery storage have been studied for their impact on grid stability. Time-varying tariffs can unintentionally synchronize loads, increasing reinforcement costs, whereas capacity-based charges help mitigate overloads by addressing potential congestion before it occurs [9]. However, many models assume uniform tariff adoption across households, overlooking the heterogeneity in consumer decision-making. Addressing this limitation, recent work has incorporated household-level tariff choices and HEMS adoption, showing that capacity-based charges can reduce reinforcement costs while influencing the adoption of dynamic tariffs [2]. While confirming the finding of increasing reinforcement costs in distribution grids with rising proliferation of dynamic tariffs under volumetric grid charges, other authors identify additional grid charge options, such as three level segmented tariffs as effective policy tool against overloads [3].

Yet, these models often simplify heat demand dynamics, not fully accounting for building thermal storage and pre-heating, which carries significant demand shifting potential [13].

In summary, existing studies highlight the significant impact of dynamic tariff adoption on overloads in distribution grids. While several studies explore grid charges as effective policy instruments for mitigation, important gaps remain in understanding how heterogeneous tariff adoption, along with detailed thermal building models that account for building thermal storage, affect model outcomes. Addressing these gaps is crucial for accurately simulating and comparing grid charge scenarios and for advancing our understanding of distribution grid overloads under various tariff schemes.

C. Contribution

Addressing the aforementioned research gaps, this paper investigates the following research question: How do different grid charge structures affect low-voltage grid stability in residential areas with increasing adoption of dynamic electricity tariffs? To answer this, we develop a simulation framework that explicitly models building thermal storage and integrates it with empirical household load data and EV charging patterns. This allows us to assess heating flexibility in household-level optimization problems, a dimension often simplified in previous studies. We aim to evaluate and compare the grid stability impacts of three grid charge schemes—volumetric, peak-level, and three-tier segmented charges—under varying dynamic tariff adoption rates. Through a case study in a suburban low-voltage grid, we analyze how these schemes mitigate transformer overloads, line congestion, and voltage issues, offering policy-relevant insights into grid charge design.

II. Research Method

The following section presents our research approach by first providing a high-level overview and then describing its different components in detail.

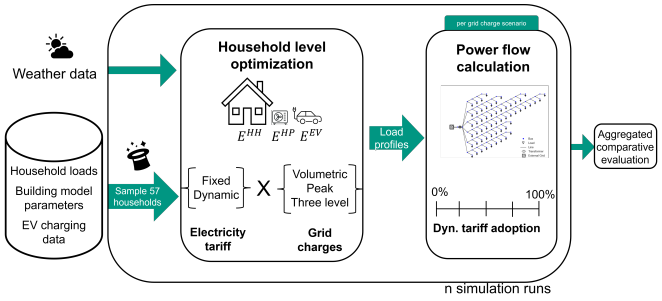

Figure 1: Methodology Overview

Figure 1 presents our three-stage approach: First, we model household-level decision-making under various pricing schemes and grid policies, where each simulation run considers a set of sampled household configurations representing a neighborhood. Second, we analyze the aggregated impact of these individual decisions on power grid operations, considering households as nodes in a low-voltage grid. Finally, we evaluate system performance through multiple simulation runs to assess grid reliability and potential overload conditions under different dynamic tariff adoption rates.

A. Monte-Carlo sampling strategy

Given that each household-level optimization problem takes multiple seconds to solve on standard hardware and a single simulation involves more than 300 such optimizations, exhaustive evaluation of all possible input parameter combinations is computationally infeasible. Instead, we employ Monte Carlo sampling, drawing building thermal characteristics based on the underlying empirical distribution of the respective house types. For all other input variables, we assume uniform distributions. This method effectively balances computational efficiency with representative system exploration [14].

B. Household-level optimization

We consider a fully electrified scenario, where each household is equipped with an EV and a heat pump, both of which are operated through a HEMS. In addition to these flexible loads, each household has an inflexible household load. In our model, operation of HEMS and controlled flexibility potentials is represented by a quadratic optimization problem. In the following, we present the underlying cost optimization problem on the household level in detail. It is based on a number of studies covering operation strategies of flexible household loads, EV charging and building thermal modelling [13], [15]–[17].

Objective function. Each household balances two competing objectives: reducing its cumulative energy costs C_t over the whole considered timespan T and maintaining occupant thermal comfort, with discomfort penalized through a term λ. This leads to the following formulation:

$$\min \sum_{t=1}^{T} (C_t) + \lambda \tag{1}$$

$$C_t = E_t \cdot p_{\mathrm{t}}, \forall t \tag{2}$$

$$E_t = E_{\mathrm{hh,t}} + E_{\mathrm{EV,t}} + E_{\mathrm{heat,t}}, \forall t \tag{3}$$

$$0 \leq E_{\mathrm{hh,t}}, E_{\mathrm{EV,t}}, E_{\mathrm{heat,t}}, \forall t \tag{4}$$

where C_t reflects the cost of procuring electricity, being the product of consumed electricity E_t with the price p_t, which may be constant or time-varying depending on the considered scenario. E_t is the sum of inflexible household electricity consumption $E_{\mathrm{hh,t}}$ and EV , $E_{\mathrm{EV,t}}$ and heat pump $E_{\mathrm{heat,t}}$ loads, both of which are flexible and governed by a set of boundary conditions elaborated in the following sections. All of these loads are non-negative at each time step.

Thermal model. The thermal model ensures occupant comfort and setpoint adherence while accurately representing the building's physical behavior. A widely adopted approach for incorporating thermal dynamics into optimization problems are resistance-capacitance models [18], which model buildings

as equivalents to electrical circuits [19]. We implement a three-resistance, two-capacitance (3R2C) thermal building model based on [13] to simulate each building's thermal behavior. We discretize via forward-euler method [20] and further extend the model by incorporating a thermal energy storage and thermal comfort component. The thermal building dynamics are governed by the following set of equations:

$$\lambda = \sum_{t=0}^{T-1} \Delta t \cdot \alpha \cdot \left(T_{\text{in},t} - \mathrm{T}_{\text{setpoint}}\right)^2 \tag{5}$$

$$T_{\text{setpoint}} \leq \sum_{t=\text{start}(d)}^{\text{end}(d)} T_{\text{in},t} \quad \forall d \in D_{\text{heating}} \tag{6}$$

$$T_{\text{in},t+1} = T_{\text{in},t} + \Delta t \Bigg[\frac{1}{C_{\text{i}} R_{\text{ie}}} \left(T_{\text{e},t} - T_{\text{in},t}\right) + \frac{1}{C_{\text{i}} R_{\text{ia}}} \left(T_{\text{out},t} - T_{\text{in},t}\right) + \frac{1}{C_{\text{i}}} \left(P_{\text{heat},t} + P_{\text{tes},t}\right) + \frac{A_{\text{i}}}{C_{\text{i}}} P_{\text{s},t} \Bigg], \forall t \in [1, T-1] \tag{7}$$

$$T_{\text{e},t+1} = T_{\text{e},t} + \Delta t \Bigg[\frac{1}{C_{\text{e}} R_{\text{ie}}} \left(T_{\text{in},t} - T_{\text{e},t}\right) + \frac{1}{C_{\text{e}} R_{\text{ea}}} \left(T_{\text{out},t} - T_{\text{e},t}\right) \Bigg], \forall t \in [1, T-1] \tag{8}$$

$$E_{\text{TES},t+1} = E_{\text{TES},t} - \Delta t P_{\text{tes},t}, \forall t \in [1, T-1] \tag{9}$$

$$P_{\text{heat},t} + P_{\text{tes},t} \geq 0, \quad \forall\, t \tag{10}$$

$$E_{\text{heat},t} = \frac{1}{COP_t} \cdot \Delta t \cdot P_{\text{heat},t}, \quad \forall\, t \tag{11}$$

where λ is the discomfort term penalizing setpoint deviations quadratically in the objective function [17]. As an additional measure for thermal comfort, we ensure that for heating days- days with an average temperature below 18°C- the average temperature does not fall under the specified setpoint, as defined in Equation (6). Equation (7) and (8) represent the thermal building model with C_i and C_e being the lumped indoor and building envelope capacitances, while R_{ie}, R_{ia} and R_{ea} are the thermal resistances between inside and envelope, inside and ambient and envelope and ambient, respectively [13]. A_i represents the effective window area. $P_{\text{s,t}}$ denotes the power of south-facing solar radiation for each time step, while $P_{\text{heat},t}$ and $P_{\text{tes},t}$ represent the average power of heat provided by the heating system and thermal energy storage at time step t. $T_{\text{in,t}}$ and $T_{\text{out,t}}$ are the indoor and outdoor temperatures at each time step. Equation (9) ensures the consistency of the thermal energy storage model, with $E_{\text{TES},t}$ denoting the storage level at time t. The thermal energy storage (TES) may only charge from the heat source, represented by Equation (10). Lastly, the electrical energy consumed for heating at each time step is subject to a time-varying coefficient of performance (COP) and the length of the time step Δt. We calculate the outdoor temperature-dependent COP as proposed by [21].

EV model. We model the flexibility of electric vehicle charging by allowing EV charging demands to be shifted within predefined sessions j characterized by a starttime, endtime, and total amount of energy charged. In addition, the charging must adhere to limits based on the maximum charging power. The flexibility of EV charging operations is governed by the following equations:

$$E_{\text{EV},t} \leq E_{\text{EV,max}}, \quad \forall t \tag{12}$$

$$\sum_{t=\text{end}(j-1)}^{\text{start}(j)} E_{\text{EV},t} = 0, \quad j \in [2, J] \tag{13}$$

$$\sum_{t=\text{start}(j)}^{\text{end}(j)} E_{\text{EV}}(t, j) = \sum_{t=\text{start}(j)}^{\text{end}(j)} E_{\text{EV,empirical,t}} \quad \forall j \in [1, J] \tag{14}$$

There, (12) enforces the energy limit per time step and (13) ensures no charging occurs outside the sessions [16]. Equation (14) guarantees that the energy demand of each session j matches the demand of the respective charging session [3].

C. Considered grid charge options

Different grid charge options are modeled by adjusting the cost term C_t as follows, with the grid term depending on the chosen grid charge option: $C_t = C_{\text{grid,t}} + E_t \cdot p_{\text{t}}, \forall t$ with $C_{\text{grid,t}}$ being the grid charges at time step t, E_t being the total energy consumption at time t and p_{t} representing the electricity price at time step t.

Volumetric grid charges. Volumetric grid charges, where customers pay a fixed fee per kWh of electricity, are a widely proliferated option [22]. It leads to the following formulation:

$$C_{\text{grid,t}} = E_t \cdot p_{\text{grid,volumetric}} \tag{15}$$

Peak pricing grid charges. The second option we model are capacity-sensitive grid charges consisting of two parts: a capacity-related peak charge billed for the maximum consumption of the billing period and a reduced volumetric grid charge. Due to incentivizing individual peak avoidance, this grid charge policy might also help to reduce aggregated peaks [2], [9]. One example of this mechanism is the grid charge policy for industrial consumers in Germany [23]. For modeling peak level grid charges in our objective function, we adjust the grid charge term as follows:

$$C_{\text{grid,t}} = \frac{1}{T} \cdot p_{\text{grid,capacity}} \cdot \max_{t \in T} E_t + p_{\text{grid,volumetric}} \cdot E_t \quad \forall t \tag{16}$$

where $p_{\text{grid,capacity}}$ represents the capacity-based grid charge, and $p_{\text{grid,volumetric}}$ denotes the volumetric grid charge. E_t represents the energy consumption at time step t.

Three-level segmented grid charges. In the case of three-level segmented grid tariffs, the volumetric price for distribution grid usage increases for additional energy with every segment [24], incentivizing flatter load profiles. It can be formulated as follows [24]:

$$C_{\text{grid,t}} = \sum_{s=1}^{S} E_t^s \cdot p_t^{\text{grid},s} \tag{17}$$

, where S represents the number of tariff segments, while E_t^s and $p_t^{\text{grid, s}}$ denote the energy consumption and the corresponding volumetric grid charge for segment s at time t, respectively.

The energy allocated to each segment is subject to the constraint:

$$0 \leq E_t^s \leq E^{s,\max}, \quad \forall s, \forall t \tag{18}$$

ensuring that it does not exceed a predefined upper limit $E^{s,\max}$. Additionally, the total household energy consumption must be met by summing over all segments:

$$E_t = \sum_{s=1}^{S} E_t^s \quad \forall t. \tag{19}$$

D. Power flow calculation

Power flows are calculated across varying adoption levels and grid charge scenarios using household-specific load patterns derived from each electricity tariff–grid charge combination. Each household's resulting load profile is mapped to a node within the modeled low-voltage distribution network. To simulate different adoption scenarios, a specified number of households are randomly selected to follow dynamic pricing load patterns, while the remainder maintain fixed-price patterns. This process is replicated across different grid charging policies, with power flow calculations performed using pandapower [25].

E. Aggregated evaluation

Three critical health parameters detect overload conditions in power systems: transformer loading, power line loading, and voltage stability. Transformer loading monitors the equipment's relative load, tracking periods when loading exceeds 100% of rated capacity, where sustained overloading accelerates transformer aging and may trigger system-wide blackouts in extreme cases [26]. Power line loading assessment identifies network congestion by comparing actual loading against line capacity; when loading exceeds rated limits, accelerated thermal degradation occurs, and severe overloads can trigger line trips, causing service interruptions [27]. Voltage stability monitoring tracks per-unit bus voltages throughout the network, with under-voltage conditions identified when values drop below 90% of the nominal value, indicating potential system instability. [28]. These fluctuations can degrade device performance and, in extreme cases, cause voltage collapse and blackouts [29].

We assess all of these parameters on an aggregated level by calculating the average over all simulation runs. To quantify uncertainty, we also compute the standard deviation for each metric.

III. Case study

This paper investigates how grid charge options influence low-voltage distribution grid overloads in a fully electrified scenario with varying adoption of dynamic pricing. The scenario considers 2019 in hourly time steps and is situated in Hamelin, Germany.

A. Empirical input data

To simulate inflexible household loads, we use empirical household load data from 2019 for multiple single-family homes located in Hamelin [30]. After filtering out houses with larger chunks of missing data, 22 load profiles were used in this study. We employ EV charging data from Norway in 2019 [31], including plug-in time, plug-out time and amount of electricity charged. After preprocessing, data from 22 chargers were used. Hourly weather data for Hamelin in 2019, including temperature and irradiance values, were sourced from Visual Crossing [32].

Dynamic electricity costs were modeled using the EPEX SPOT day-ahead prices for 2019, obtained from the ENTSO-E Transparency Platform API [33]. For the fixed price scenario, we calculated a daily consumption-weighted average of the wholesale price. This fixed price consequently excludes any risk premiums potentially reflected in standard fixed-price contracts.

B. Thermal model parameters

To model heating demand, we employ a 3R2C thermal model. We derive the required parameters of thermal resistance, capacitance, and effective window area from [13]. These values are available for a set of representative German single-family homes. The study also provides heating power specifications and estimates the prevalence of each building type in the German housing stock [13]. We use these prevalence estimates to establish the distribution of building types across our house archetypes (detailed in Appendix A), which informs our sampling methodology. In addition, we assume each house to be equipped with a 500 l thermal energy storage, amounting to roughly 20 kWh of storage capacity, which can be discharged in one hour [34]. The setpoint is constantly set to 21°C and α, the discomfort coefficient to 0.05.

C. Low-voltage grid model

We model the grid in Pandapower using the Kerber village network [35], which is frequently used in studies investigating residential low-voltage distribution grids [28], [36], [37]. The Kerber network includes 116 buses, 57 loads, 114 lines, a transformer, and a grid connection, with "NAYY 150" cables for main lines and "NAYY 50" for branchout lines.

D. Parametrization of grid charges

Based on empirical data from 2024, volumetric grid charges of 0.115 €/kWh [38] were used. For peak load grid charges, the peak price component is set to 67.94 €/kW, following empirical data [39]. To ensure revenue neutrality compared to the volumetric-only scenario when no optimization is applied, we adjust the volumetric price component of our peak grid charges accordingly. This results in an average volumetric charge component of 0.025 €/kWh.

For three-level grid charges, the pricing structure is defined as follows: The first segment applies to consumption up to the average hourly household consumption. The second segment covers consumption up to three times the average and is priced twice as high as the first. The third segment applies to consumption beyond this threshold and is priced ten times higher than the first. To maintain comparability, we set the price of the first segment so that the grid operator's revenue remains unchanged when applying the base case load data.

IV. Results

In this section, we discuss the aggregated results of 30 simulation runs of the case study investigating a fully electrified scenario of 57 households in Hamelin.

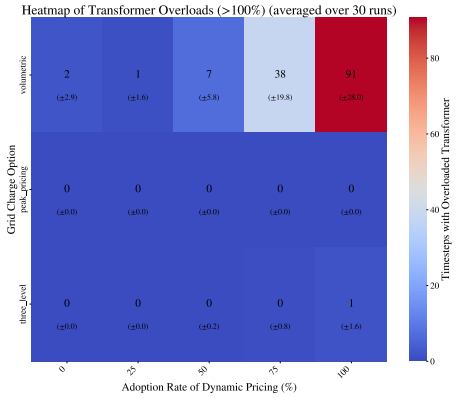

Figure 2: Hours with transformer overloads per adoption sand grid policy scenario

Figure 2 represents the observed hourly time steps with transformer overloads averaged over the 30 simulation runs. While for volumetric grid charges, only single instances of overloads occur for dynamic tariff adoption rates below 50%, they dramatically increase with further rising adoption rates, reaching over 90 hours with transformer overloads in case of full dynamic tariff adoption. In contrast, overloads can be almost entirely averted with the other grid charge policies, with only one overload occurring on average with three-level grid charges and full dynamic tariff adoption. A similar pattern emerges when considering hours with elevated transformer load (depicted in Appendix B). While those increase with rising adoption rates across all grid charge policies, they are by far the highest in the volumetric grid charge case.

With respect to the remaining overload metrics, which are depicted in the appendix, the aforementioned pattern holds true: With rising adoption rates of dynamic prices, the stress on the grid increases. However, the effect is alleviated in the case of peak and three-level grid charges. Critical overloads are only observed with volumetric grid charges. Overall, peak pricing grid charges appear to be slightly more effective in stabilizing the grid than three-level grid charges.

V. Discussion and Conclusion

This study advances the understanding of grid charge structures by incorporating a detailed building heat model into the analysis of fully electrified residential scenarios. While previous work has established the effectiveness of different grid charge approaches in electrified settings [2], [3], our analysis uniquely accounts for the thermal dynamics of buildings and their impact on flexibility potential. Our findings show that both peak-level and three-tier segmented charges maintain grid stability when households optimize across heat pumps, electric vehicles, and building thermal mass, while volumetric charges prove insufficient at high adoption rates of dynamic electricity tariffs. Our results extend existing research in two key ways. First, by incorporating detailed thermal building physics, we demonstrate how the interaction between building characteristics and heating system operation affects the overall effectiveness of different grid charge structures. Second, we show that the benefits of peak-level and segmented charges persist even when accounting for realistic thermal constraints and comfort requirements. These insights are particularly relevant as they provide a more nuanced understanding of flexibility potential in residential heating systems. The disparity between our simulation results and empirical findings from existing networks [40] suggests that realizing the potential of sophisticated grid charges requires concurrent advancement in household automation systems, particularly in thermal management. This observation highlights the importance of coordinating grid charge policy with smart home technology deployment. While our findings are specific to the German context, the effectiveness of peak-level and three-tier charges would likely extend to other regions experiencing similar electrification trends, though performance may vary with climate conditions and building characteristics. Limitations of our study include the exclusion of photovoltaic systems and battery storage, reliance on a single grid topology, and use of data from a period of relatively stable electricity prices. Future work should examine how these factors influence outcomes across diverse geographic and regulatory contexts.

In conclusion, our findings provide grid operators and policymakers with new insights into how building thermal storage influences the effectiveness of different grid charge structures. The results suggest that peak-level or segmented charges can effectively manage grid stability even when accounting for realistic thermal constraints.

Acknowledgment

The authors would like to thank their colleagues from the Institute for Information Systems (WIN) for the fruitful discussions.

References

[1] European Parliament and Council, *Directive (EU) 2019/944 of the European Parliament and of the Council of 5 June 2019 on common rules for the internal market for electricity and amending Directive 2012/27/EU (recast)*, Official Journal of the European Union, L 158, 14.6.2019, p. 125–199, Text with EEA relevance, 2019. [Online]. Available: https://eur-lex.europa.eu/eli/dir/2019/944/oj/eng.

[2] J. Stute and M. Klobasa, "How do dynamic electricity tariffs and different grid charge designs interact? - Implications for residential consumers and grid reinforcement requirements," *Energy Policy*, vol. 189, p. 114 062, Jun. 2024, ISSN: 0301-4215. DOI: 10.1016/j.enpol.2024.114062. (visited on 01/24/2025).

[3] L. Semmelmann, K. Kaiser, A. Heider, K. J. Kircher, G. Hug, and C. Weinhardt, "Analyzing the impact of dynamic tariff adoption and regulatory options on distribution grids with an open-source framework [unpublished manuscript]," in *Proceedings of the ACM International Conference on Future and Sustainable Energy Systems (ACM e-Energy '25)*, Rotterdam, Netherlands, 2025.

[4] European Union, *Directive (eu) 2023/2413 of the european parliament and of the council of 18 october 2023 on the promotion of the use of energy from renewable sources*, Accessed: 2025-02-01, 2023. [Online]. Available: https://eur-lex.europa.eu/legal-content/EN/TXT/?uri=CELEX%3A32023L2413.

[5] International Energy Agency, *Renewables*, Accessed: 2025-01-30, 2023. [Online]. Available: https://www.iea.org/energy-system/renewables.

[6] International Energy Agency, *Tracking clean energy progress 2023*, https://www.iea.org/reports/tracking-clean-energy-progress-2023, Licence: CC BY 4.0, 2023.

[7] S. Bellocchi, M. Manno, M. Noussan, M. G. Prina, and M. Vellini, "Electrification of transport and residential heating sectors in support of renewable penetration: Scenarios for the Italian energy system," *Energy*, vol. 196, p. 117 062, Apr. 2020, ISSN: 0360-5442. DOI: 10.1016/j.energy.2020.117062. (visited on 01/29/2025).

[8] B. Zhou, W. Li, K. W. Chan, *et al.*, "Smart home energy management systems: Concept, configurations, and scheduling strategies," *Renewable and Sustainable Energy Reviews*, vol. 61, pp. 30–40, Aug. 2016, ISSN: 1364-0321. DOI: 10.1016/j.rser.2016.03.047. (visited on 02/01/2025).

[9] L. Kundert, A. Heider, and G. Hug, "The Influence of Different Network Tariffs on Distribution Grid Reinforcement Costs," in *2023 IEEE Belgrade PowerTech*, Jun. 2023, pp. 1–6. DOI: 10.1109/PowerTech55446.2023.10202875. (visited on 01/24/2025).

[10] S. A. Steinbach and M. J. Blaschke, "How grid reinforcement costs differ by the income of electric vehicle users," *Nature Communications*, vol. 15, no. 1, p. 9674, Nov. 2024, ISSN: 2041-1723. DOI: 10.1038/s41467-024-53644-0. (visited on 01/24/2025).

[11] Y. Li and A. Jenn, "Impact of electric vehicle charging demand on power distribution grid congestion," *Proceedings of the National Academy of Sciences*, vol. 121, no. 18, e2317599121, Apr. 2024. DOI: 10.1073/pnas.2317599121. (visited on 02/08/2025).

[12] A. Lilienkamp and N. Namockel, "Integrating EVs into distribution grids — Examining the effects of various DSO intervention strategies on optimized charging," *Applied Energy*, vol. 378, p. 124 775, Jan. 2025, ISSN: 0306-2619. DOI: 10.1016/j.apenergy.2024.124775. (visited on 01/28/2025).

[13] E. Sperber, U. Frey, and V. Bertsch, "Reduced-order models for assessing demand response with heat pumps – Insights from the German energy system," *Energy and Buildings*, vol. 223, p. 110 144, Sep. 2020, ISSN: 0378-7788. DOI: 10.1016/j.enbuild.2020.110144. (visited on 01/24/2025).

[14] A. Shapiro, "Monte Carlo Sampling Methods," in *Handbooks in Operations Research and Management Science*, ser. Stochastic Programming, vol. 10, Elsevier, Jan. 2003, pp. 353–425. DOI: 10.1016/S0927-0507(03)10006-0. (visited on 02/02/2025).

[15] T. Hubert and S. Grijalva, "Modeling for Residential Electricity Optimization in Dynamic Pricing Environments," *IEEE Transactions on Smart Grid*, vol. 3, no. 4, pp. 2224–2231, Dec. 2012, ISSN: 1949-3061. DOI: 10.1109/TSG.2012.2220385. (visited on 02/07/2025).

[16] M. Müller, Y. Blume, and J. Reinhard, "Impact of behind-the-meter optimised bidirectional electric vehicles on the distribution grid load," *Energy*, vol. 255, p. 124 537, Sep. 2022, ISSN: 0360-5442. DOI: 10.1016/j.energy.2022.124537. (visited on 02/07/2025).

[17] S. Salakij, N. Yu, S. Paolucci, and P. Antsaklis, "Model-Based Predictive Control for building energy management. I: Energy modeling and optimal control," *Energy and Buildings*, vol. 133, pp. 345–358, Dec. 2016, ISSN: 0378-7788. DOI: 10.1016/j.enbuild.2016.09.044. (visited on 02/07/2025).

[18] S. Prívara, J. Cigler, Z. Váňa, F. Oldewurtel, C. Sagerschnig, and E. Žáčeková, "Building modeling as a crucial part for building predictive control," *Energy and Buildings*, vol. 56, pp. 8–22, Jan. 2013, ISSN: 0378-7788. DOI: 10.1016/j.enbuild.2012.10.024. (visited on 08/22/2024).

[19] J. Drgoňa, J. Arroyo, I. Cupeiro Figueroa, *et al.*, "All you need to know about model predictive control for buildings," *Annual Reviews in Control*, vol. 50, pp. 190–232, Jan. 2020, ISSN: 1367-5788. DOI: 10.1016/j.arcontrol.2020.09.001. (visited on 06/14/2024).

[20] H. İ. Tol and H. B. Madessa, "Development of a white-box dynamic building thermal model integrated with a heating system," *Journal of Building Engineering*, vol. 68, p. 106 038, Jun. 2023, ISSN: 2352-7102. DOI: 10.1016/j.jobe.2023.106038. (visited on 02/07/2025).

[21] C. Verhelst, F. Logist, J. Van Impe, and L. Helsen, "Study of the optimal control problem formulation for modulating air-to-water heat pumps connected to a residential floor heating system," *Energy and Buildings*, vol. 45, pp. 43–53, Feb. 2012, ISSN: 0378-7788. DOI: 10.1016/j.enbuild.2011.10.015. (visited on 02/04/2025).

[22] Q. Hoarau and Y. Perez, "Network tariff design with prosumers and electromobility: Who wins, who loses?" *Energy Economics*, vol. 83, pp. 26–39, Sep. 2019, ISSN: 0140-9883. DOI: 10.1016/j.eneco.2019.05.009. (visited on 02/09/2025).

[23] Bundesnetzagentur, *Monitoringbericht energie 2024*, Accessed: 2025-01-30, 2024. [Online]. Available: https://data.bundesnetzagentur.de/Bundesnetzagentur/SharedDocs/Mediathek/Monitoringberichte/MonitoringberichtEnergie2024.pdf.

[24] N. Li, K. Bruninx, and S. Tindemans, "Residential demand-side flexibility provision under a multi-level segmented tariff," in *2023 IEEE PES Innovative Smart Grid Technologies Europe (ISGT EUROPE)*, Oct. 2023, pp. 1–5. DOI: 10.1109/ISGTEUROPE56780.2023.10407675. (visited on 01/30/2025).

[25] L. Thurner, A. Scheidler, F. Schafer, *et al.*, "Pandapower - an open source python tool for convenient modeling, analysis and optimization of electric power systems," *IEEE Transactions on Power Systems*, 2018, ISSN: 0885-8950. DOI: 10.1109/TPWRS.2018.2829021. [Online]. Available: https://arxiv.org/abs/1709.06743.

[26] M. Aslam, I. U. Haq, M. S. Rehan, *et al.*, "Health Analysis of Transformer Winding Insulation Through Thermal Monitoring and Fast Fourier Transform (FFT) Power Spectrum," *IEEE Access*, vol. 9, pp. 114 207–114 217, 2021, ISSN: 2169-3536. DOI: 10.1109/ACCESS.2021.3104033. (visited on 01/29/2025).

[27] S. Liu, C. Cruzat, and K. Kopsidas, "Impact of transmission line overloads on network reliability and conductor ageing," in *2017 IEEE Manchester PowerTech*, Jun. 2017, pp. 1–6. DOI: 10.1109/PTC.2017.7980857. (visited on 01/30/2025).

[28] R. S. Singh, G. Mier, T. Bosma, M. Eijgelaar, G. Bloemhof, and G. Sauba, "Assessment of EV charging strategies and their effect on residential grids using co-simulation," in *2022 International Conference on Smart Energy Systems and Technologies (SEST)*, Sep. 2022, pp. 1–6. DOI: 10.1109/SEST53650.2022.9898417. (visited on 01/30/2025).

[29] R. Verayiah, A. Mohamed, H. Shareef, and I. Z. Abidin, "Review of under-voltage load shedding schemes in power system operation," *Przegląd elektrotechniczny*, vol. 90, no. 7, pp. 99–103, 2014. DOI: 10.12915/pe.2014.07.19.

[30] M. Schlemminger, T. Ohrdes, E. Schneider, and M. Knoop, "Dataset on electrical single-family house and heat pump load profiles in Germany," *Scientific Data*, vol. 9, no. 1, p. 56, Feb. 2022, ISSN: 2052-4463. DOI: 10.1038/s41597-022-01156-1. (visited on 01/27/2025).

[31] Å. L. Sørensen, K. B. Lindberg, I. Sartori, and I. Andresen, "Residential electric vehicle charging datasets from apartment buildings," *Data in Brief*, vol. 36, p. 107 105, Jun. 2021, ISSN: 2352-3409. DOI: 10.1016/j.dib.2021.107105. (visited on 01/27/2025).

[32] Visual Crossing, *Weather data services*, https://www.visualcrossing.com/, Accessed: 2025-01-10. Data provided by Visual Crossing Weather., 2025.

[33] ENTSO-E, *Entso-e transparency platform*, https://transparency.entsoe.eu/, Accessed via API on: 2024-12-23, 2025.

[34] C. Finck, R. Li, R. Kramer, and W. Zeiler, "Quantifying demand flexibility of power-to-heat and thermal energy storage in the control of building heating systems," *Applied Energy*, vol. 209, pp. 409–425, Jan. 2018, ISSN: 0306-2619. DOI: 10.1016/j.apenergy.2017.11.036. (visited on 02/09/2025).

[35] G. Kerber, "Aufnahmefähigkeit von Niederspannungsverteilnetzen für die Einspeisung aus Photovoltaikkleinanlagen," Ph.D. dissertation, Technische Universität München, 2011.

[36] C. Gehbauer and J. Müller, "Hierarchical multi-level electric power system simulation with smart photovoltaic systems using the functional mock-up interface on the lawrencium computing cluster," in *Proceedings of the American Modelica Conference*, 2020, pp. 120–129. DOI: 10.3384/ecp20169120.

[37] E. Elliott, N. Shanklin, S. Zehtabian, Q. Zhou, and D. Turgut, "Peer-to-Peer Energy Trading and Grid Impact Studies in Smart Communities," in *2020 International Conference on Computing, Networking and Communications (ICNC)*, Feb. 2020, pp. 674–678. DOI: 10.1109/ICNC47757.2020.9049665. (visited on 02/01/2025).

[38] BDEW Bundesverband der Energie- und Wasserwirtschaft e.V., *BDEW-Strompreisanalyse Dezember 2024*, Accessed: 2025-01-27, Dec. 2024. [Online]. Available: https://www.bdew.de/service/daten-und-grafiken/bdew-strompreisanalyse/.

[39] Avacon Netz GmbH, *Preisliste der netzentgelte für den zugang zum stromnetz*, Accessed: 2025-02-04, 2018. [Online]. Available: https://www.avacon-netz.de/content/dam/revu-global/avacon-netz/documents/netzentgelte-strom/2019/avang_strom_01012019preisblaetterstand14122018.pdf.

[40] F. El Gohary, B. Stikvoort, and C. Bartusch, "Evaluating demand charges as instruments for managing peak-demand," *Renewable and Sustainable Energy Reviews*, vol. 188, p. 113 876, Dec. 2023, ISSN: 1364-0321. DOI: 10.1016/j.rser.2023.113876. (visited on 01/24/2025).

APPENDIX A
INPUT OF THE MONTE CARLO SIMULATION

For our Monte Carlo sampling, we used established RC-Parameters for the German building stock [13]. Figure 3 represents the relative frequencies we used for the sampling of the different building types. For each building type, there are three different parameter sets depending on the renovation state of the building. For the renovation state, a uniform distribution was assumed.

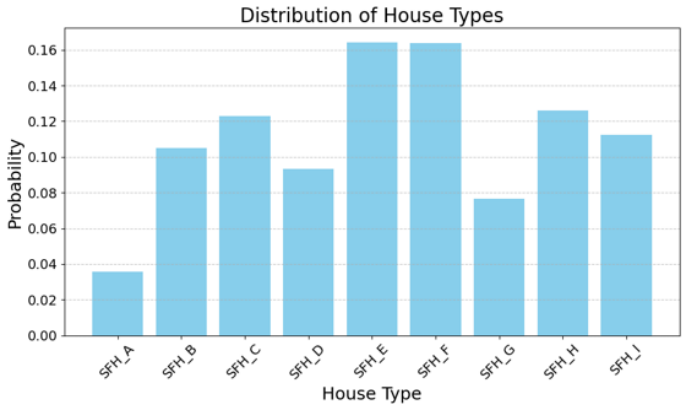

Figure 3: Relative frequencies of considered house types

APPENDIX B
FURTHER OVERLOAD METRICS CONSIDERED IN THIS STUDY

The following visualizations provide a more detailed overview of the three overload metrics we tracked in this study: transformer load, line overloads and voltage limit violations.

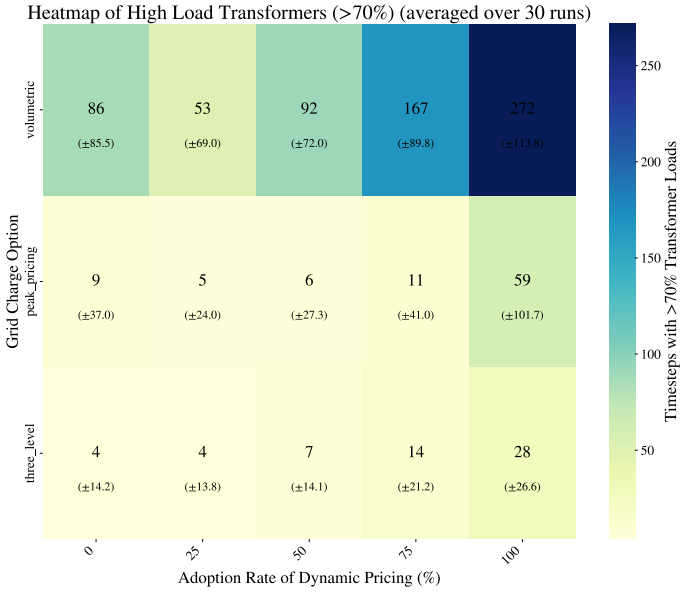

Figure 4: Hours with transformer loads >70% per adoption and grid policy scenario

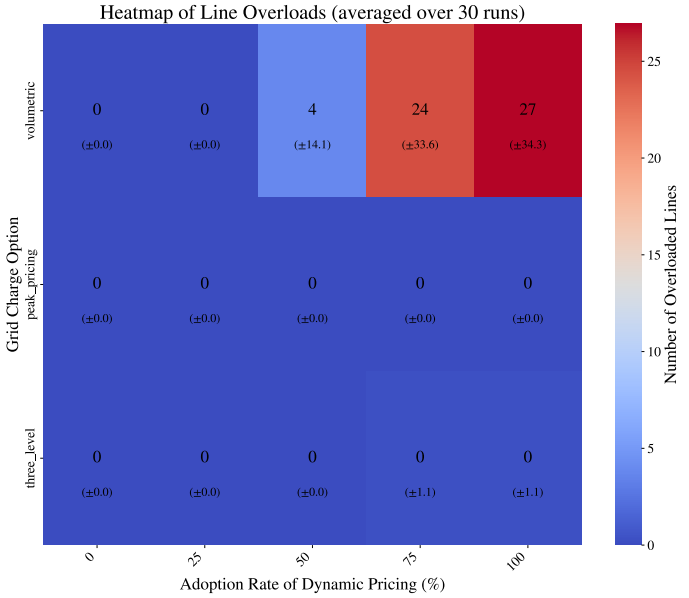

Figure 5: Hours with line overloads per adoption and grid policy scenario

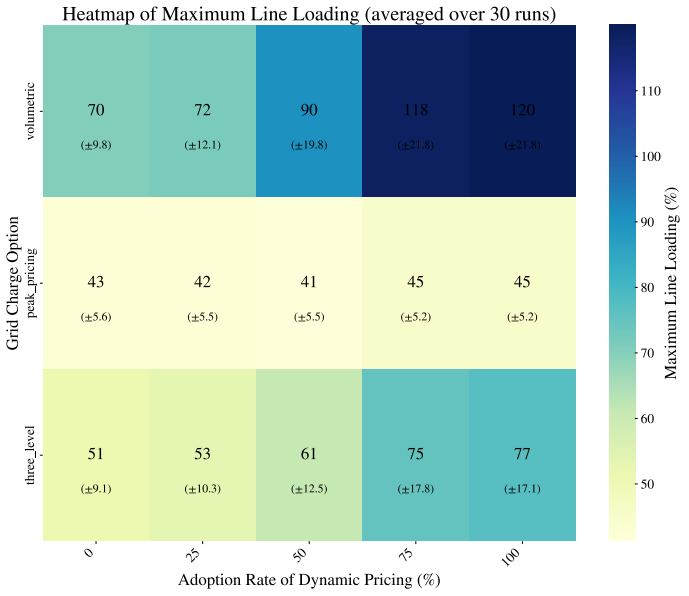

Figure 6: Maximum line loading observed per adoption and grid policy scenario

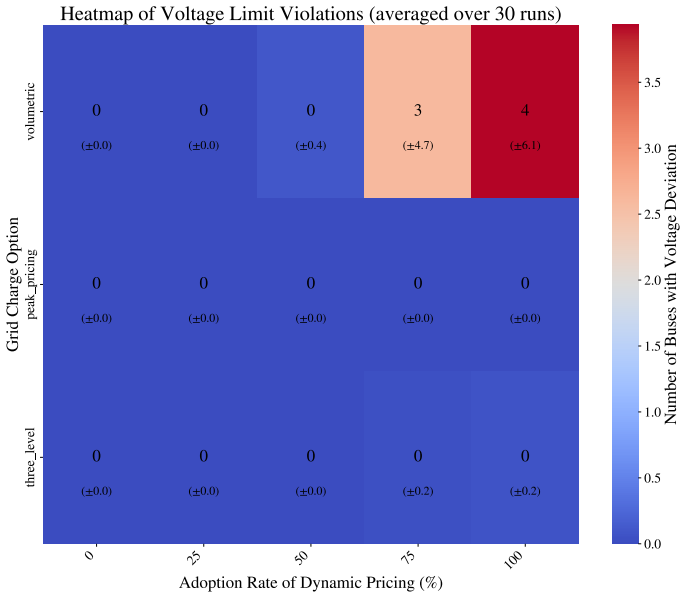

Figure 7: Hours with voltage limit violations per adoption and grid policy scenario

Figure 8: Minimum voltage levels per adoption and grid policy scenario